



## APPENDIX AVAILABLE ON THE HEI WEB SITE

### Research Report 167

#### **Assessment and Statistical Modeling of the Relationship Between Remotely Sensed Aerosol Optical Depth and PM<sub>2.5</sub> in the Eastern United States**

**Christopher J. Paciorek and Yang Liu**

#### **Appendix B. Additional Analysis of Spatio-Temporal Associations between GOES Aerosol Optical Depth Retrievals and Ground-Level PM<sub>2.5</sub>**

---

Correspondence may be addressed to Dr. Christopher J. Paciorek, Department of Statistics, 367 Evans Hall, University of California, Berkeley, CA 94720; e-mail: [paciorek@stat.berkeley.edu](mailto:paciorek@stat.berkeley.edu).

Although this document was produced with partial funding by the United States Environmental Protection Agency under Assistance Award CR-83234701 to the Health Effects Institute, it has not been subjected to the Agency's peer and administrative review and therefore may not necessarily reflect the views of the Agency, and no official endorsement by it should be inferred. The contents of this document also have not been reviewed by private party institutions, including those that support the Health Effects Institute; therefore, it may not reflect the views or policies of these parties, and no endorsement by them should be inferred.

This document was reviewed by the HEI Health Review Committee but did not undergo the HEI scientific editing and production process.

© 2012 Health Effects Institute, 101 Federal Street, Suite 500, Boston, MA 02110-1817

## B. Additional Analysis of Spatio-temporal Associations between GOES Aerosol Optical Depth Retrievals and Ground-level PM<sub>2.5</sub>

### B.1. Data availability and raw correlations

Defining potential retrievals as those occurring at times with solar zenith angle less than 70°, Fig. B1 shows the spatial pattern of available retrievals for the U.S. There are few retrievals satisfying the criteria in the northern US during fall and winter, due to high levels of cloudiness and surface reflectivity. During summer and spring, the spatial differences in availability occur at small spatial scales. Note that during spring and summer, the number of potential retrievals in each season is relatively constant across the eastern United States, but for fall and winter, the number of potential retrievals in each season ranges from approximately 1400 in the extreme south (southern Florida) to 600 in the extreme north (northern Minnesota).

Fig. B2 shows the retrieval success by time of day and season for locations in the eastern U.S. (east of 85° W to focus on an area in a single time zone). This indicates that there are pronounced daily cycles with a low proportion of retrievals at mid-day compared to morning and afternoon.

Fig. B3 shows temporal correlations across space separately for all four seasons. The results are similar to the full-year results (Fig. 1), although with some indication of low correlations in the southeastern U.S. in the spring.

### B.2. Time series estimates of daily AOD and associated uncertainty

One estimate of daily AOD is the simple arithmetic average of the available AOD retrievals. Section 3 focuses on this estimate because of its simplicity and because the estimator described below does not substantially improve the calibration, as discussed in Section B.3. However, in other settings, accounting for correlation in estimating long-term averages may be important. Here we outline the approach.

The disadvantage of using the simple arithmetic average is that it does not account for the temporal correlations between half-hourly values. Standard statistical theory indicates that a better estimator (one with less variability) can be obtained by accounting for the correlations and that an estimate of the uncertainty of the estimated daily average AOD should account for the temporal correlation as well.

We want to estimate the integrated AOD across the time period during which observations are available. Letting  $a(h)$  represent AOD as a function of the time of day, we wish to estimate

$$a_d = \frac{1}{|t_2 - t_1|} \int_{t_1}^{t_2} a(h) dh \text{ for each day } d.$$

In spatial statistics the best linear unbiased predictor (BLUP) of the integrated value is the so-called block-kriging estimator, which relies on calculating covariances between intervals and single points in time (when applied to this temporal setting).

A numerical approximation is to predict  $a(h)$  at a set of times, say a fine grid of times covering the interval  $(t_1 = t_{min} - 15\text{min}, t_2 = t_{max} + 15\text{min})$  where  $t_{min}$  and  $t_{max}$  are the first and last times that the solar zenith angle is less than  $70^\circ$  and where we extend the time window by half the time interval between observation times (15 minutes) so that all prediction times are within 15 minutes of a possible retrieval. We then approximate the integral as the average of the predictions at each time point on the fine grid based on a time series model

$$\hat{a}_d = \frac{1}{N} \sum_{i=1}^N \hat{a}(h_i)$$

where  $\hat{a}(h_i)$  is the BLUP for AOD at time  $h_i$ . The BLUP must account for the correlation between AOD at different times; by doing so, the prediction  $\hat{a}(h_i)$  is a weighted average of AOD values from nearby times. The overall estimator weights observations that are widely separated from other observations more than observations for which the most recent and nearest times in the future have available AOD values, as these provide somewhat redundant information. After exploratory analysis using time series of AOD for days with at least 10 observations, an AR(1) time series model appears appropriate for most days and locations. It appears that the autoregressive parameter in the AR(1) model varies slightly as a function of the number of AOD observations available but  $\rho = 0.3$  seems to be a good compromise value for the correlation between observations one-half hour apart. This correlation is lower than one would expect for the true aerosol optical depth over time; we suspect the low autocorrelation is due to noisiness in the satellite-retrieved AOD as an estimate of true AOD. The kriging model assumes the AOD observations over time at the prediction grid times (which include the observation times as well) follow a normal distribution,  $a \sim N(\mu \mathbf{1}, \sigma^2 \Sigma)$  where  $\Sigma_{ij} = \rho^{2|h_i - h_j|}$ . The prediction,  $\hat{a} = (\hat{a}(h_1), \dots, \hat{a}(h_N))$ , takes the form of the simple kriging estimator (Schabenberger and Gotway 2005),

$$\begin{aligned} \hat{a} &= \hat{\mu} \mathbf{1}_p + \Sigma_{21} \Sigma_{11}^{-1} (a_{\text{present}} - \hat{\mu} \mathbf{1}_n) \\ \hat{\mu} &= (\mathbf{1}_n^\top \Sigma_{11}^{-1} \mathbf{1}_n)^{-1} \mathbf{1}_n^\top \Sigma_{11}^{-1} a_{\text{present}} \end{aligned} \quad (\text{B1})$$

where  $\mathbf{1}_n$  is an  $n$ -vector of ones and  $\Sigma_{11}$  is the correlation matrix (a submatrix of  $\Sigma$ ) for the available data,  $a_{\text{present}}$ .  $\Sigma_{21}$  is the correlation between the predictions at the fine grid of times and the times of the available data and is calculated in the same manner as  $\Sigma_{11}$ . Following R. Smith (UNC Department of Statistics, unpublished), one can also derive the full prediction covariance matrix as

$$\begin{aligned} V(\hat{a}) &\propto \Sigma_{22} - \Sigma_{21} \Sigma_{11}^{-1} \Sigma_{12} + (\mathbf{1}_p^\top \Sigma_{11}^{-1} \mathbf{1}_p)^{-1} \\ &(\mathbf{1}_p \mathbf{1}_p^\top - \mathbf{1}_p \mathbf{1}_n^\top \Sigma_{11}^{-1} \Sigma_{12} - (\mathbf{1}_p \mathbf{1}_n^\top \Sigma_{11}^{-1} \Sigma_{12})^\top + (\Sigma_{21} \Sigma_{11}^{-1} \mathbf{1}_n)(\Sigma_{21} \Sigma_{11}^{-1} \mathbf{1}_n)^\top) \end{aligned} \quad (\text{B2})$$

where  $\Sigma_{22} = \Sigma$  is the correlation between all the prediction times on the fine grid. The proportionality comes from leaving out a term,  $\sigma^2$ , common to all the predictions. Our estimate of  $\hat{a}_d$  has variance proportional to  $\frac{1}{N^2} \mathbf{1}_p^\top V(\hat{a}) \mathbf{1}_p$ , which we use as our estimate,  $V(\hat{a}_d)$ .

Because of the relatively low autocorrelation of  $\rho = 0.3$  between half-hourly values, the

resulting estimates of  $\hat{a}_d$  do not vary substantially from  $\bar{a}_d$ , though the relative variances (ignoring  $\sigma^2$ ) are somewhat different than  $1/n$ , the variance estimator for  $\bar{a}_d$  (also ignoring  $\sigma^2$ ).

### B.3. Model selection process

To arrive at the final model (3.1), we considered a variety of models, comparing models based on qualitative assessment of the fitted smooth functions and on quantitative comparison of the cross-validated correlations of calibrated AOD with PM<sub>2.5</sub>.

In Section 3, we used the simple arithmetic average,  $\bar{a}_{it}$ , with homoscedastic (i.e., constant variance) error. As an alternative, we first consider a model that uses the more sophisticated time series-based estimator of daily AOD,  $\hat{a}_{it}$  (B1):

$$\log \hat{a}_{it} \sim N(\mu + g(s_i) + f_t(t) + f_{\text{PBL}}(\text{PBL}_{it}) + f_{\text{RH}}(\text{RH}_{it}) + \beta \text{PM}_{it}, \sigma^2 V(\hat{a}_{it}) + \tau^2). \quad (\text{B3})$$

This approach accounts for the pattern of missing retrievals using weighting derived from the autocorrelation structure, downweighting retrievals that are close in time to other retrievals and upweighting retrievals that are isolated from other retrievals. The heteroscedastic variance accounts for the varying levels of certainty in the daily AOD estimates caused by having different numbers of AOD retrievals in a day (and by the time pattern of available retrievals).  $V(\hat{a}_{it})$  is derived in (B2).  $\tau^2$  accounts for the inherent noise in the relationship between AOD and PM<sub>2.5</sub> that would be present even without any missing retrievals. The term  $\sigma^2$  is the proportionality constant that is missing from (B2) and, with  $\tau^2$ , is estimated in the model fitting. Table B1 (column (c)) includes a tabulation of the correlations from the time series approach for comparison with calibration based on the simple arithmetic average. The correlations improve only marginally and fitting (B3) is much more computationally intensive, so the final model in Section 3 used the simple arithmetic average.

To investigate whether linearity in the relationship of PM<sub>2.5</sub> to AOD is a reasonable assumption and to consider whether using PM<sub>2.5</sub> or log PM<sub>2.5</sub> in the model is preferable, we compared models with the same format as the final model but using a smooth regression function of pollution, either  $f_{\text{PM}}(\text{PM}_{it})$  or  $f_{\log \text{PM}}(\log \text{PM}_{it})$  in place of  $\beta \text{PM}_{it}$ . We found a reasonably linear relationship of  $\log \bar{a}_{it}$  with PM<sub>2.5</sub> on the original scale while the association of  $\log \bar{a}_{it}$  with log PM<sub>2.5</sub> was not linear, which would complicate the construction of the calibration model (3.2-3.3). Further justifying the linearity of PM<sub>2.5</sub> in the final model, the model using  $f_{\text{PM}}(\text{PM}_{it})$  explained only slightly more of the variability in  $\log \bar{a}_{it}$  than when using the linear term.

The final model fits  $f_t(t)$  as a smooth function of time, with about four effective degrees of freedom for each season. We also fit a model allowing a much less smooth function of time, which can account for short-term changes in the relationship between AOD and PM<sub>2.5</sub>. This model overfits, with lower correlations between calibrated AOD and PM<sub>2.5</sub> (about 0.04 lower than those shown in Table B1). We also considered removing  $f_t(t)$  from the model entirely. This change slightly reduced correlations compared to the final model. While we continue to include time in the model, we note that accounting for temporally-varying bias seems to be of

limited importance, probably because any factors that change the relationship over time do not affect the entire eastern U.S. all at once, while  $f_i(t)$  can only represent changes over time affecting the entire spatial domain.

Next we considered different approaches to including the meteorological functions in the model. In the basic model, we used the average of RH and PBL over UTC times 12:00, 15:00, 18:00, and 21:00 to roughly match the time range of AOD retrievals. We also considered the use of RH and PBL as the average of only using UTC times 15:00 and 18:00 and as the value only at UTC time 18:00, to more closely match the period of maximum PBL during each day (PBL increases rapidly during late morning, so times of 15:00 and 18:00 are generally the highest values during a given 24-hour period). Both of these specifications had very little effect on the correlations, nor did using log PBL (following Liu et al. 2005) in place of PBL.

We also considered a simplified model with only a spatial bias function,

$$\log \bar{a}_{it} \sim N(\mu + g(s_i) + \beta \text{PM}_{it}, \tau^2). \quad (\text{B4})$$

which has the benefit of not requiring one to obtain meteorological information for the calibration. Table B1 demonstrates that the simple model performs well compared to the final model. While Fig. 3 and model assessment results (not shown) indicate that time, RH and PBL are significant predictors of AOD, they do not explain enough variability in AOD such that the calibration model improves substantially by including these functions. The much greater importance of the spatial function than the meteorological functions may be related to the confounding effect we discuss in Section 3.

Spatial variation in the relationship between AOD and  $\text{PM}_{2.5}$  may be related to varying reflectivity, particularly between rural, vegetated areas and urban areas. As a proxy for reflectivity, we considered adding smooth regression functions of road density and population density but found they had little impact on the model fit, with the functions estimated to be essentially flat, indicating no relationship with AOD. Road and population density were calculated as follows. In the larger project of which this is a part, we have divided the eastern U.S. into four km square grid cells and estimated the population density in each cell from the 2000 U.S. Census, as well as the density of roads in each cell based on the ESRI StreetMap 9.2 product. Using the cell whose centroid was closest to the AOD pixel centroid, we assigned road and population density estimates to each matched pair. This level of aggregation serves to reflect local land use characteristics, which seems appropriate for the AOD data at the pixel resolution, but may not be the most appropriate for capturing fine-scale features that affect  $\text{PM}_{2.5}$  concentrations at monitors.

We considered whether the multiplicative bias,  $\beta$  in the final model, might vary spatially, fitting the model

$$\log \bar{a}_{it} \sim N(\mu + g(s_i) + f_i(t) + f_{\text{PBL}}(\text{PBL}_{it}) + f_{\text{RH}}(\text{RH}_{it}) + (\beta + \beta(s_i))\text{PM}_{it}, \tau^2) \quad (\text{B5})$$

fitting an average effect,  $\beta$ , and also a spatially-varying bias,  $\beta(s)$ . This model can also be fit with the `gam()` function in R, but we note that one should be cautious with such a model because of the potential non-identifiability in distinguishing  $g(s)$  from  $\beta(s)$ . The fitted model indicates that there is substantial spatially-smooth variation in the multiplicative scaling, with the standard deviation of the fitted  $\beta(s)$  across the sites equal to 0.0049, 0.0043 and 0.0068 for spring,

summer and fall respectively, which is substantial variation relative to the estimates,  $\hat{\beta}$ , of 0.016, 0.016, and 0.013 for the three seasons. Fig. B4 shows the estimates of  $g(s)$  and  $\beta + \beta(s)$ , with evidence that the spatial patterns change somewhat between seasons. The overall patterns in the additive spatial function are similar to those estimated in the base model with the lower than expected AOD over the Appalachian Mountains/Ohio Valley, while the variability in the multiplicative scaling shows no particular interpretable pattern. Based on the multiplicative model, one could try to use the following calibration

$$a_{it}^* = \frac{1}{\hat{\beta} + \hat{\beta}(s)} \left( \log \bar{a}_{it} - \hat{\mu} - \hat{g}(s_i) - \hat{f}_t(t) - \hat{f}_{\text{PBL}}(\text{PBL}_{it}) - \hat{f}_{\text{RH}}(\text{RH}_{it}) \right).$$

However, when  $\hat{\beta} + \hat{\beta}(s) \approx 0$ , the model is indicating there is little relationship between AOD and  $\text{PM}_{2.5}$  and there are some extreme calibrated values,  $a_{it}^*$ . Instead, in our use of calibrated AOD in the larger project, we plan to allow for spatially-varying multiplicative bias directly in the statistical model rather than in the calibration step used to preprocess the AOD retrievals.

#### B.4. Assessing the usefulness of AOD observations of uncertain quality

The processing of AOD retrievals produces a number of quality flags that may be used to screen out retrievals of poor quality, which might be biased or merely very noisy estimates of true AOD. These standard criteria used by NOAA to screen the retrievals are to require the following conditions for a valid retrieval: AOD value less than 10, AOD standard deviation less than 0.15, surface reflectivity greater than 0.01 and less than 0.15, channel 1 visible reflectivity greater than zero, aerosol signal greater than 0.01, and no clouds detected by the cloud screening in a 5 by 5 array of cells centered on the pixel of interest (Cloudsum=25). In addition, our analyses make use of the data from times and locations with a solar zenith angle less than  $70^\circ$ . Retrievals are generally less accurate at high zenith angle, as is the case for other remote sensing techniques, because of limitations of the plane-parallel radiative transfer model (Dahlback and Stamnes 1991), which ignores the earth's curvature.

Given the availability of the gold standard  $\text{PM}_{2.5}$  data, for which we would like GASP AOD to serve as a proxy, we can consider relaxing or making more stringent these standard quality criteria. The goal is to see if stronger associations with  $\text{PM}_{2.5}$  can be obtained, or if equivalent associations can be obtained but with an increase in the number of usable retrievals. Note that we need to be cautious of finding stronger associations with stricter criteria merely because the stricter criteria result in removing AOD- $\text{PM}_{2.5}$  pairs that while less strongly associated are still associated with  $\text{PM}_{2.5}$ , which in a statistical prediction model would amount to throwing away proxy data with useful, albeit more variable, information. Since our focus is on potential relaxation of the criteria, we address this by comparing correlations calculated based only on matched pairs for days with at least one AOD retrieval under the stricter standard criteria.

We consider relaxing the following individual quality flag criteria one at a time: 1.) AOD standard deviation less than 0.30 rather than 0.15; 2.) Cloudsum > 20 rather than Cloudsum=25; 3.) Cloudsum > 15 rather than Cloudsum=25; 4.) solar zenith angle <  $75^\circ$  rather than zenith angle <  $70^\circ$ ; 5.) solar zenith angle <  $80^\circ$ ; 6.) solar zenith angle <  $85^\circ$ ; 7.) surface reflectivity < 20 rather than < 15; and 8.) surface reflectivity < 25. Comparing only matched pairs for days

with at least one AOD under the standard criteria, Table B2 shows correlations of AOD and  $PM_{2.5}$  for the various criteria, excluding winter. The results suggest that relaxing the standard deviation criterion produces lower associations; this criterion serves to screen out retrievals when neighboring pixels have very different retrieved values, potentially because of cloud contamination. In contrast, relaxing the cloudsum criterion has limited effect when more than 20 of the pixels in the surrounding 5 by 5 array are cloud free, suggesting little information is added or lost from augmenting daily AOD averages based on these additional retrievals. Further relaxation of the cloudsum criterion appears to result in loss of information. Relaxing the surface reflectivity criterion decreases correlations. In contrast, relaxing the zenith angle criterion increases the associations between the AOD proxies and  $PM_{2.5}$ . Even relaxing so far as to include observations with zenith angle less than  $85^\circ$  seems to increase associations in all but the yearly averaging, for which the association decreases but not significantly so. One note of caution is that Prados et al. (2007) found higher mean square error in GASP AOD compared to AERONET AOD early and late in the day compared to the middle of the day (although correlations were no lower during these times), providing empirical evidence that GASP AOD may be less accurate as a estimate of AOD at high solar zenith angles.

Table B3 shows the increase in the number of retrievals and the number of days with several thresholds for the number of retrievals under the various criteria, indicating that the relaxed criteria admit a sizable increase in retrievals.

We can also consider correlations between AOD and  $PM_{2.5}$  for new matched pairs that become available when relaxing the criteria, namely locations for which there was no AOD retrieval on the day under the stricter criteria. These new matched pairs are almost always based on a single AOD retrieval during the day, so a point of comparison is the correlation between the calibrated AOD under the standard criteria and  $PM_{2.5}$  for days with only one matched pair, which is 0.38. The correlations for the new matched pairs are 0.37 and 0.35 when increasingly relaxing the cloudsum criterion; 0.30 when relaxing the standard deviation criterion; 0.33, 0.33, and 0.27 when increasingly relaxing the zenith angle criterion; and 0.26 in both cases of relaxing the reflectivity criterion. Given the calibration results in Table B2, it's somewhat surprising that relaxing the cloudsum criterion seems to outperform relaxing the zenith angle criterion when considering only new daily observations made available because of the relaxed criteria. In all cases, the positive correlations suggest that there is information about  $PM_{2.5}$  available in the discarded observations that do not satisfy the standard criteria.

Next we consider making the zenith angle criteria more strict. Not surprisingly given that relaxing this criteria seems worthwhile, making it more strict decreased the correlations between the AOD proxies and  $PM_{2.5}$  (generally by about 0.02). We also considered setting all negative AOD values to zero or excluding negative observations, the latter following Prados et al. (2007). Setting the negative values to zero slightly decreased correlations while excluding such observations markedly decreased correlations (generally by about 0.04), so we suggest using the negative values as reported rather than truncating or excluding them when one's goal is use of AOD as a proxy for  $PM_{2.5}$ .

## References

Dahlback A, Stamnes K. 1991. A new spherical model for computing the radiation field available for photolysis and heating at twilight. *Planetary and Space Science* 39: 671–683.

Liu Y, Sarnat JA, Kilaru V, Jacob DJ, Koutrakis P. 2005. Estimating ground-level PM<sub>2.5</sub> in the eastern United States using satellite remote sensing. *Environmental Science and Technology* 39: 3269–3278.

Prados AI, Kondragunta S, Ciren P, Knapp KR. 2007. GOES aerosol/smoke product (GASP) over North America: comparisons to AERONET and MODIS observations. *Journal of Geophysical Research-Atmospheres* 112: D15201.

Schabenberger O, Gotway CA. 2005. *Statistical Methods for Spatial Data Analysis*. Chapman & Hall, Boca Raton.

**Table B1. Correlations between various GASP AOD proxies and  $PM_{2.5}$  at different temporal resolutions in the eastern U.S. in 2004, excluding winter. The four AOD proxies are: (a) raw AOD, calculated using the log average daily AOD; (b) calibrated AOD (3.2) in Section 3 based on  $\bar{a}_i$ ; (c) calibrated AOD (B3) based on  $\hat{a}_i$  from a time series model (B1); and (d) calibrated AOD (B4) based on  $\bar{a}_i$  from the simplified model without time, PBL and RH. Correlations are shown both when using matched pairs for days with any number of AOD retrievals and restricting to days with at least five retrievals.**

temporal resolution of correlations	(a) Raw AOD ( $\log \bar{a}_i$ )	(b) Calibrated AOD ( $a_i^*$ ) using $\log \bar{a}_i$	(c) Calibrated AOD ( $a_i^*$ ) using $\log \hat{a}_i$	(d) Calibrated AOD ( $a_i^*$ ) based on (B4)
	any number of AOD retrievals in a day			
daily	0.41	0.50	0.51	0.50
monthly averages (at least 3 matched days for each site-month)	0.34	0.62	0.63	0.63
yearly averages (at least 10 matched days for each site)	0.17	0.75	0.76	0.74
	at least five AOD retrievals each day			
daily	0.51	0.59	0.60	0.60
monthly averages (at least 3 matched days for each site-month)	0.41	0.67	0.69	0.67
yearly averages (at least 10 matched days for each site)	0.19	0.69	0.71	0.67

**Table B2. Correlations between GASP AOD and PM<sub>2.5</sub> under different criteria for AOD validity for different temporal resolutions for the eastern U.S. in 2004. All values are based on matched pairs for which there is at least one daily retrieval under the strictest (the standard) criteria. p-values from paired t-tests are indicated as (\*) p<0.01; (\*\*) p<0.001; (\*\*\*) p<0.0001. Each test compares the squared model residuals from the regression of PM<sub>2.5</sub> on the AOD proxy based on the standard criteria (i.e., the top row results) to the squared model residuals from the regression of PM<sub>2.5</sub> on the AOD proxy based on one of the alternative criteria, to see if the mean squared residuals are substantially different under the alternative criteria. The monthly and yearly columns are based on calibrated AOD.**

	daily, raw AOD	daily, calibrated AOD	monthly averages (at least 3 matched days for each site-month)	yearly averages (at least 10 matched days for each site)
Standard criteria	0.408	0.502	0.617	0.745
Relax std. dev. criterion	0.402*	0.486***	0.598***	0.743
Relax Cloudsum criteria (>20)	0.411*	0.502	0.617	0.746
Further relax cloudsum (>15)	0.410	0.498*	0.612	0.738
Relax zenith angle (<75°)	0.423***	0.520***	0.629***	0.747
Further relax zenith angle (<80°)	0.428***	0.530***	0.638***	0.751
Further relax zenith angle (<85°)	0.427***	0.532***	0.637***	0.739
Relax reflectivity criterion (<20)	0.379**	0.494***	0.600***	0.722***
Relax reflectivity criterion (<25)	0.379**	0.492***	0.594***	0.716***

**Table B3. Percentage increase in number of retrievals under different criteria for GASP AOD validity in the eastern U.S. in 2004, excluding winter, all compared to the standard criteria. Note that these only reflect retrievals that match PM<sub>2.5</sub> data and are meant only to give a rough estimate of the effect of the criteria on the number of retrievals.**

	Number of half-hourly retrievals	Number of days with at least one retrieval	Number of days with at least three retrievals	Number of days with at least five retrievals
Relax std. dev. criterion	21	11	10	42
Relax Cloudsum criterion (>20)	9	11	7	33
Further relax Cloudsum (>15)	13	15	11	38
Relax zenith angle (<75°)	14	11	9	38
Further relax zenith angle (<80°)	24	15	15	49
Further relax zenith angle (<85°)	34	23	20	58
Relax reflectivity criterion (<20)	24	14	15	50
Relax reflectivity criterion (<25)	28	15	17	54

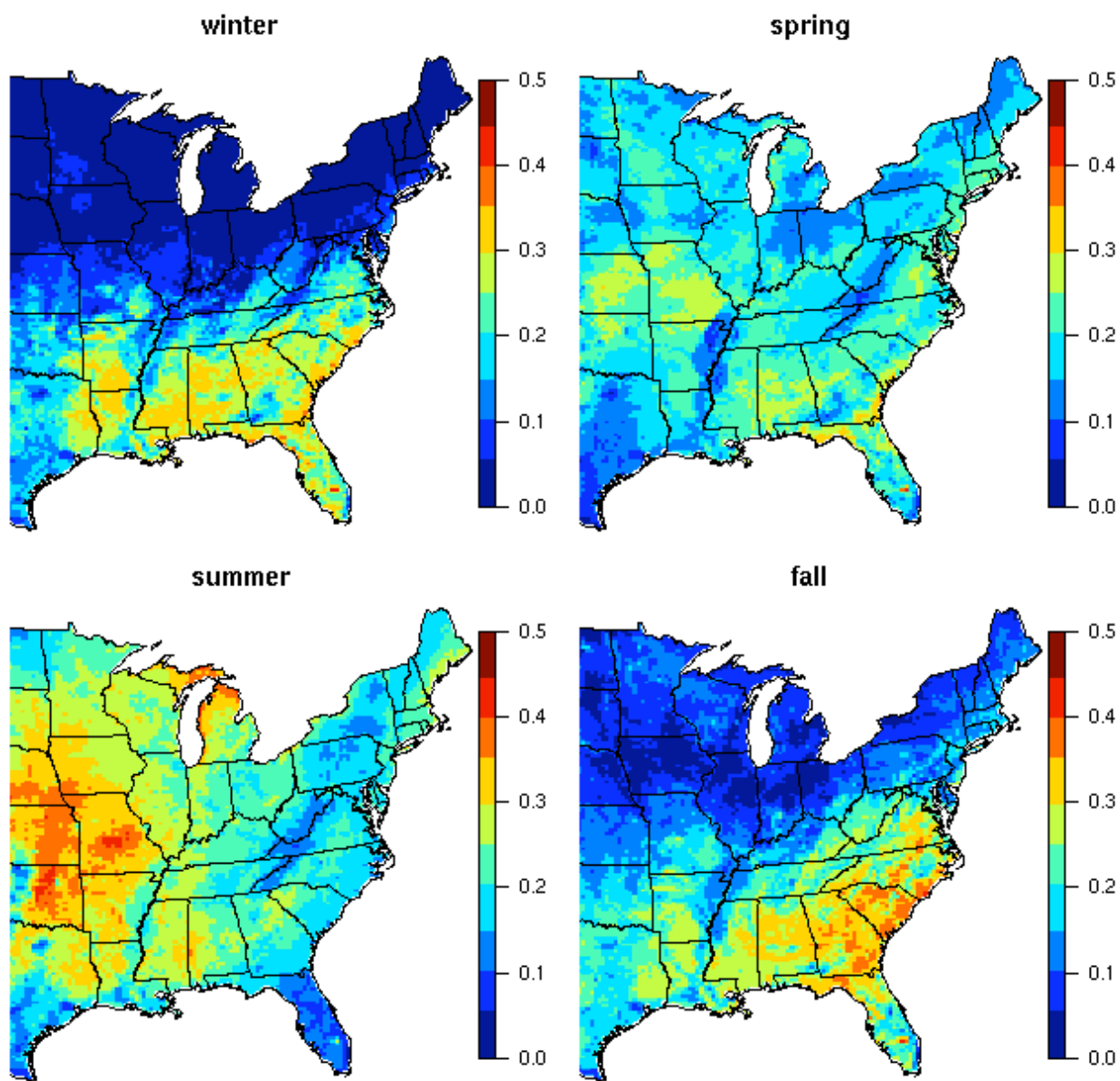
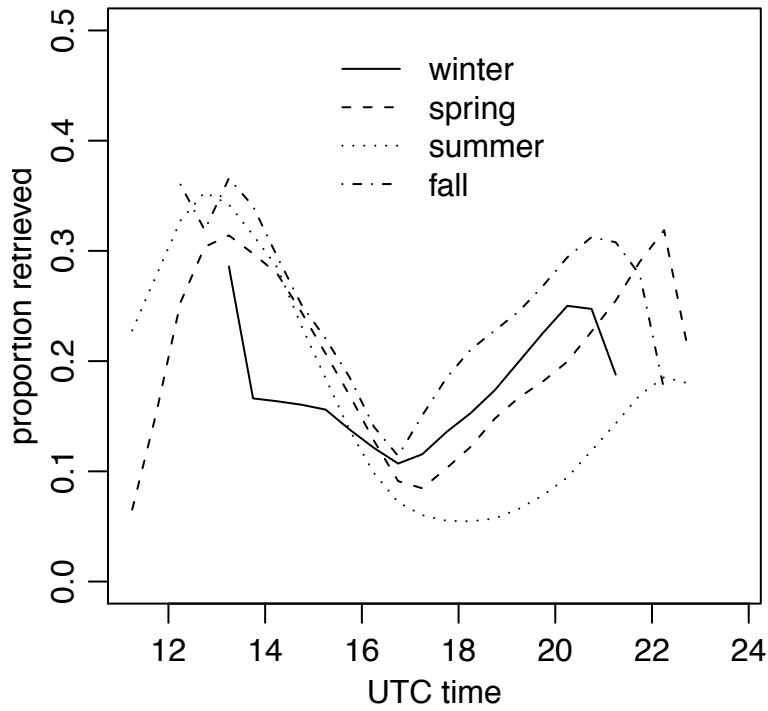
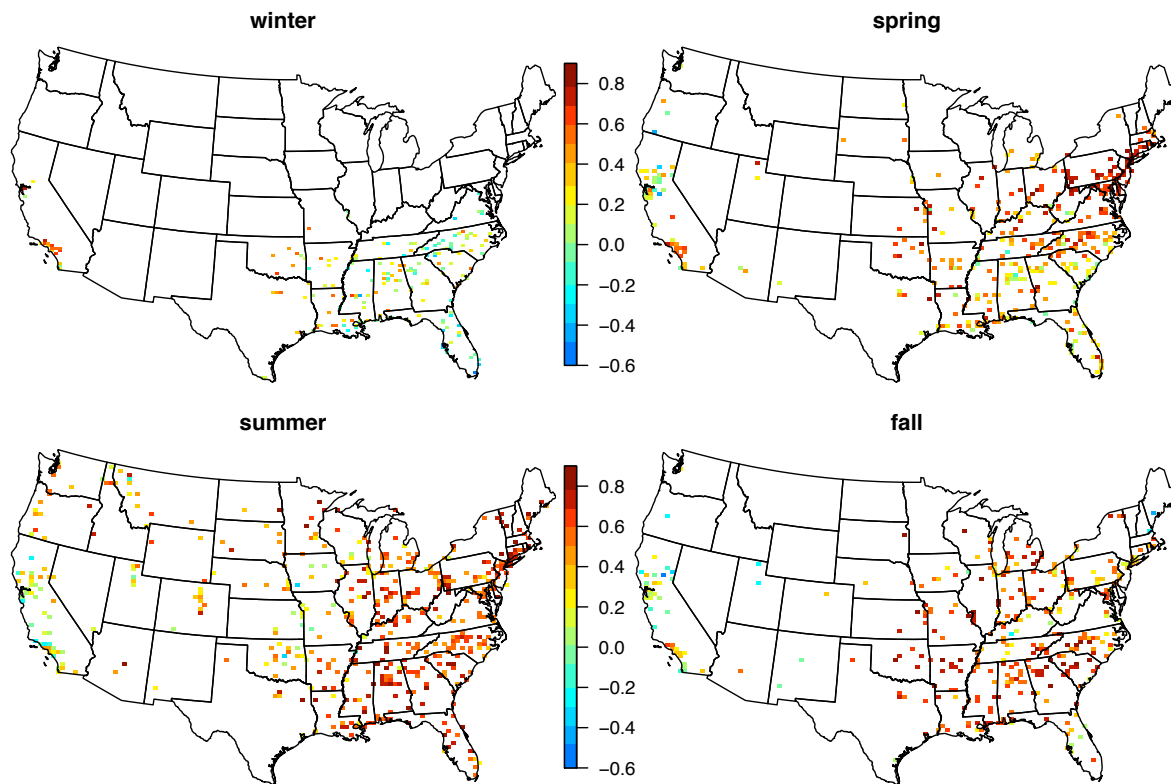


Figure B1. The proportion of potential GASP AOD retrievals by season that satisfy the GASP AOD screening criteria in 2004. A potential retrieval is defined as one with solar zenith angle less than  $70^\circ$ .



**Figure B2. Proportion of potential GASP AOD retrievals (defined as those with solar zenith angle less than 70°) that satisfy the GASP AOD screening criteria, by season in the eastern U.S. in 2004. Decreased retrieval success at the beginning and end of the day for spring and summer are in part a function of NOAA's data storage and reporting system.**



**Figure B3. Temporal correlations at individual sites between daily average  $PM_{2.5}$  and the average of half-hourly GASP AOD retrievals by season for 2004. Plots are based on site-days with at least three AOD retrievals, and only locations with at least 10 days of matched pairs are shown.**

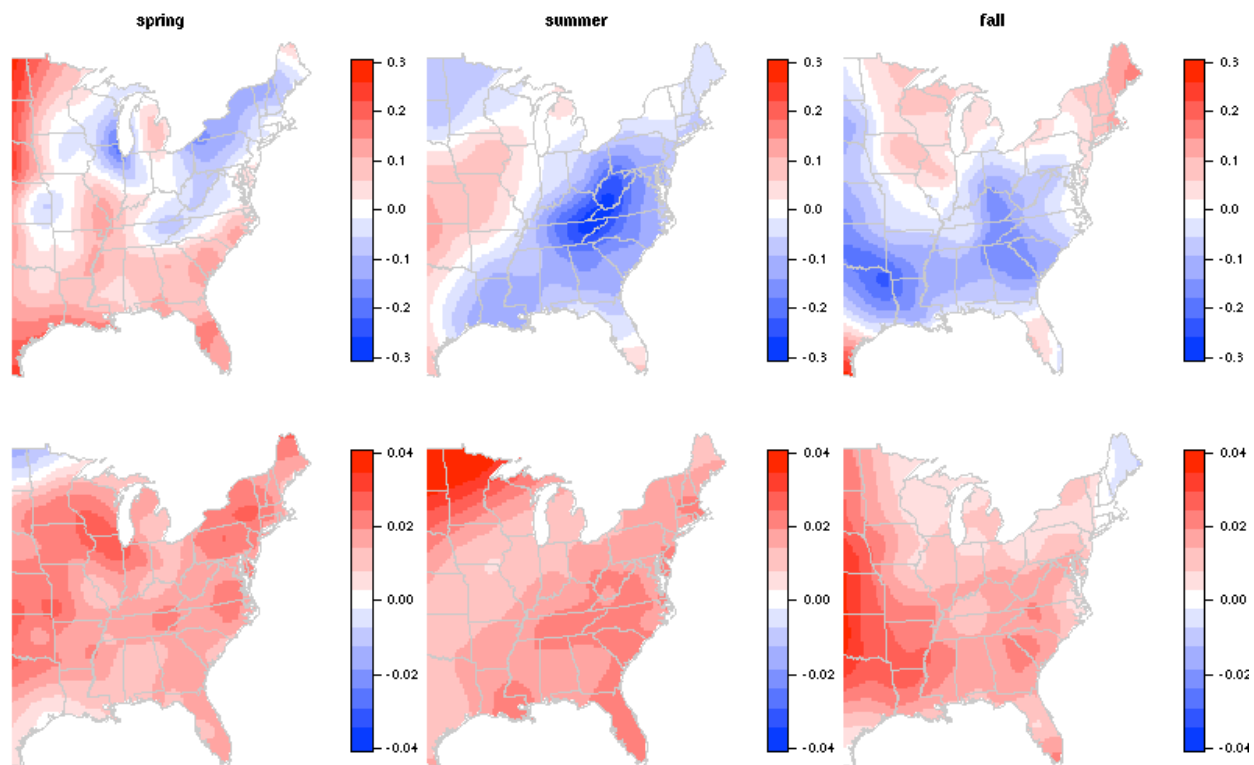


Figure B4. Fitted spatial functions for model (B5) by season: additive functions,  $\hat{g}(s)$  (top row) and multiplicative scaling functions,  $\hat{\beta} + \hat{\beta}(s)$  (bottom row). In the grayscale version the '<' symbols indicate areas with negative values.